EARTH SURFACE PROCESSES AND LANDFORMS
Earth Surf. Process. Landforms (2013)

Published online in Wiley Online Library
(wileyonlinelibrary.com) DOI: 10.1002/esp.3366

Letters to ESEX

Topographic structure from motion: a new development in photogrammetric measurement

Mark A. Fonstad,[1]* James T. Dietrich,[1] Brittany C. Courville,[2] Jennifer L. Jensen[2] and Patrice E. Carbonneau[3]
[1] Department of Geography, University of Oregon, Eugene, OR 97403 USA
[2] Department of Geography, Texas State University, TX 78666 USA
[3] Department of Geography, Durham University, Durham, UK

Received 12 December 2011; Revised 29 October 2012; Accepted 1 November 2012

*Correspondence to: Mark A. Fonstad, Department of Geography, University of Oregon, Eugene, OR 97403 USA. E-mail: fonstad@uoregon.edu

ESPL
Earth Surface Processes and Landforms

ABSTRACT: The production of topographic datasets is of increasing interest and application throughout the geomorphic sciences, and river science is no exception. Consequently, a wide range of topographic measurement methods have evolved. Despite the range of available methods, the production of high resolution, high quality digital elevation models (DEMs) requires a significant investment in personnel time, hardware and/or software. However, image-based methods such as digital photogrammetry have been decreasing in costs. Developed for the purpose of rapid, inexpensive and easy three-dimensional surveys of buildings or small objects, the 'structure from motion' photogrammetric approach (SfM) is an image-based method which could deliver a methodological leap if transferred to geomorphic applications, requires little training and is extremely inexpensive. Using an online SfM program, we created high-resolution digital elevation models of a river environment from ordinary photographs produced from a workflow that takes advantage of free and open source software. This process reconstructs real world scenes from SfM algorithms based on the derived positions of the photographs in three-dimensional space. The basic product of the SfM process is a point cloud of identifiable features present in the input photographs. This point cloud can be georeferenced from a small number of ground control points collected in the field or from measurements of camera positions at the time of image acquisition. The georeferenced point cloud can then be used to create a variety of digital elevation products. We examine the applicability of SfM in the Pedernales River in Texas (USA), where several hundred images taken from a hand-held helikite are used to produce DEMs of the fluvial topographic environment. This test shows that SfM and low-altitude platforms can produce point clouds with point densities comparable with airborne LiDAR, with horizontal and vertical precision in the centimeter range, and with very low capital and labor costs and low expertise levels. Copyright © 2012 John Wiley & Sons, Ltd.

KEYWORDS: structure from motion; topographic modeling; digital elevation models; LiDAR

Introduction

The production of high-resolution topographic datasets is of increasing interest and application throughout the geomorphic sciences (Butler *et al.*, 2001; Hancock and Willgoose, 2001; Lane, 2003; Bird *et al.*, 2010; Fonstad and Marcus, 2010). A wide range of topographic measurement methods have evolved to meet this production need, such as terrestrial laser scanning, aerial LiDAR, multibeam SONAR, RTK GPS, and total station surveys (Heritage and Hetherington, 2007; Alho *et al.*, 2009; Notebaert *et al.*, 2009; Brasington, 2010; Höfle and Rutzinger, 2011; Hohenthal *et al.*, 2011). Despite the range of available methods, the production of high resolution, high quality digital elevation models (DEMs) generally requires a significant investment in personnel time, hardware and/or software (Marcus and Fonstad, 2008). Image based methods, such as digital photogrammetry (Chandler, 1999; Lane, 2000; Butler *et al.*, 2002; Chandler *et al.*, 2002; Baily *et al.*, 2003; Carbonneau *et al.*, 2003; Lane *et al.*, 2003; Westaway *et al.*, 2003; Gimenez *et al.*, 2009; Marzolff and Poesen, 2009; Lane *et al.*, 2010), have steadily been decreasing in costs. Photogrammetry is becoming accessible to a wider base of users following the development of methods allowing for the accurate calibration of non-metric cameras and the increasingly reliable automation of the photogrammetric process (Chandler, 1999; Chandler *et al.*, 2002; Carbonneau *et al.*, 2003). Recent developments should lower the cost of image based topography even further. Initially developed for the purpose of rapid, inexpensive and easy three-dimensional surveys of buildings or small objects, the Structure from Motion approach (SfM) is an image-based surface restitution method which relies on the most recent, automated, image-to-image registration methods. When compared with classic digital photogrammetry, the use of the latest image matching algorithms in the SfM workflow leads to a much higher level of automation and much greater ease of use. In this communication

we demonstrate that SfM can deliver data quality and resolutions which are comparable with LiDAR and classic photogrammetry but with an unprecedented ease of use and with a very low cost. We therefore argue that SfM could deliver a methodological leap forward if transferred to the geomorphic sciences.

A full review of the SfM process is not appropriate for this manuscript and we refer the reader to Snavely *et al*. (2006, 2008) and Snavely (2008) for more discussion of this computer vision process. However, we shall give a brief, qualitative, overview of the SfM workflow. Similarly to traditional (i.e. classic) photogrammetry, SfM uses images acquired from multiple viewpoints in order to restitute the three-dimensional geometry of an object or surface. However, SfM diverges significantly from traditional photogrammetry. The main fundamental difference between SfM and classic photogrammetry is the use of a new generation of image matching algorithms which allow for unstructured image acquisition. While classic photogrammetric methods typically rely on strips of overlapping images acquired in parallel flight lines, SfM was designed to restitute the three-dimensional geometry of buildings and objects from randomly acquired images. As in the case of classic photogrammetry, the only caveat is that each physical point on the restituted object be present in multiple images. The usability of randomly positioned imagery is based on progress in the area of automated image matching (e.g. the scale invariant feature transform (SIFT) of Lowe, 1999). One crucial property of these new image matching approaches is their ability to recognize conjugate features (a physical feature present in many images) in multiple images despite the presence of large changes in image scale (i.e. resolution) and large changes in view point. This is a significant advance when compared with the kernel-based image correlation approaches used in classic digital photogrammetry. These kernel-based approaches rely on a cross-correlation, usually calculated with a simple image convolution operator, between pixel patches extracted from two images. As a result, these cross-correlation methods are very sensitive to changes in image resolution. In contrast, algorithms such as the SIFT key developed by Lowe (1999) rely on multiscale image brightness and colour gradients in order to identify points in the image which can reliably be identified as conjugate. The use of multiple scales in the SIFT key means that mixed image resolutions are no longer an issue. Furthermore, the use of gradients instead of absolute pixel values means that an object seen from multiple viewpoints can still be identified thanks to colour gradient between the object and its background.

Another fundamental difference between SfM and classic digital photogrammetry is the point in the workflow at which real-world map coordinates and elevations are introduced. In classic photogrammetry, the collinearity equations which describe the relationship between a three- dimensional object and its projection onto a two-dimensional image (Wolf and Dewitt, 2000) are solved *after* the user identifies and inputs ground control points (GCPs) of known positions and/or camera positions and orientations. More recent and advanced implementations of digital photogrammetry, such as *BAE systems Socet Set* as used in Miller *et al*. (2009), can solve the collinearity equations before the identification of GCPs. This approach is very similar to the SfM approach described below thus highlighting the fact that developments in SfM and classic photogrammetry are not divergent. However, we would argue that the majority of practitioners and researchers in traditional photogrammetry, as well as the bulk of published literature (Lane, 2000; Carbonneau *et al*., 2003; Rango *et al*., 2009; Smith *et al*., 2009), still follow the classic photogrammetric approach where the collinearity equations are solved *after* the input of GCPs. In order to solve these equations, the theoretical minimum requirement is three ground control points with known X, Y and Z positions, or the six camera parameters giving the X, Y and Z position along with the three rotation angles at the time of image acquisition. In practice, a larger number of ground control points, in excess of six per image overlap, are used and the over-determination of the collinearity equations is optimally resolved with a least-squares bundle adjustment. Additionally, extra GCPs are commonly used in traditional photogrammetry in order to calibrate the focal length and lens distortion parameters of the camera. This camera calibration is an essential step in the photogrammetric workflow. Once the cameras are calibrated and the collinearity equations solved in a least-squares sense, a kernel-based image matching approach is generally used to determine conjugate points in the images which are then converted into elevations via the solved collinearity equations. In the kernel-based matching process, the solution to the collinearity equations is used to constrain the search area for conjugate points. As a result, errors in the GCPs can ultimately propagate to the final resulting topography in both linear and non-linear ways. Furthermore, errors in the kernel-based matching approach can add another source of non-linear error. Contrastingly, in the SfM workflow, the collinearity equations are always solved *before* the introduction of real-world coordinates. As a result of the large number of conjugate points identified during the automated image matching phase, SfM can solve the collinearity equations in an arbitrarily scaled coordinate system. Furthermore, recent implementations of SfM also include a full camera calibration which is made possible by the large number of conjugate points (readers should, however, consult Chandler *et al*., 2003 concerning limitations of earlier SfM approaches). The intermediate stage in the SfM workflow is therefore a relative point cloud of X, Y and Z positions which is not registered to any real-world coordinate system. At this point, the user must introduce GCPs and/or camera positions in order to transform and register this SfM point cloud to an established map coordinate system, or to a local coordinate system, with a seven-parameter transformation having one scale parameter, three translation parameters and three rotation parameters. This transformation is linear and rigid and yields a point-cloud suited for mapping applications.

Readers should note the implication of the different approaches used by SfM and traditional photogrammetry. In traditional photogrammetry, the final quality of the generated topography relies on a relatively small number (<100) of highly accurate and precise GCPs and/or camera positions. These points allow for the calibration of the camera and for a high quality reconstruction of 3D geometry. Since the GCPs are used to solve the collinearity in object space (i.e. real-world space), field-measurement errors in the GCP propagate to this solution and this effect can be non-linear if the distribution of GCP errors is not random. In SfM, the final quality of the camera calibration and of the point-cloud relies on a very large number (>1000) of automatically generated conjugate points in the images which have varying degrees of error that are hidden from the user and are a function of image properties. Since the final registration of this SfM point-cloud relies on a purely linear transformation, any non-linear distortions introduced by errors in the automated matching process cannot be removed. Furthermore, additional, linear, errors can be introduced in the SfM process by low quality GCPs leading to errors in the seven-parameter transform. There is therefore an assumption in SfM that the automated image matching process yields precise and accurate results with little non-linear deformation. This is a crucial assumption that still needs rigorous testing and verification.

However, the initial experience of a range of users and their results are very encouraging. The SfM workflow has significantly more automation and thus is perceived by users as being much more straightforward and simple. This ease of use has been greatly enhanced in recent years by the development of freely available software such as Microsoft Photosynth and Bundler and low-cost commercial packages such as Photoscan by Agisoft Inc. and 123D Catch by Autodesk Inc. Verhoeven (2009) and Verhoeven *et al.* (2009) have conducted introductory tests of the modern SfM process using low-altitude helikites in archaeology. A handful of other recent SfM applications to topography have been presented previously at professional conferences and published in abstracts and proceedings (Dietrich, 2010; Dietrich *et al.*, 2011; Fonstad *et al.*, 2011a, 2011b, 2011c). Dowling *et al.* (2009) used SfM and a hand-held camera to study soil erosion over a 1 m^2 plot. Templeton *et al.* (2010) used an unmanned aerial system (UAS) helicopter and SfM to generate DEMs for ecohydrological research. Welty *et al.* (2010) used hand-held camera images taken from a plane to construct the topography of the Columbia Glacier. While these authors show SfM DEMs that are remarkably easy to produce and visually stunning, the uncertainties and limitations of this new method are only partially known. Such errors can profoundly influence uses of these DEMs in geomorphology, such as in sediment budgeting (Wheaton *et al.*, 2010). The purpose of this article is to introduce the method to geomorphologists, provide a proof-of-concept investigation of the SfM approach to produce realistic topographic point clouds, and to show that DEMs produced from the point clouds are of reasonably comparable quality to DEMs made from aerial LiDAR. This short article is not intended as a full quantitative test of the accuracy and precision capabilities of the SfM; such tests will be required in the different domains of geomorphology in the future for inclusion of this approach into the science.

Assessment of Topographic Accuracy

Study area

We chose to investigate the SfM approach at Pedernales Falls State Park in Texas, USA because it provides a highly diverse topographic landscape in a small area. The Pedernales River in this park is primarily a bedrock-controlled river with strong jointing. This has created an abruptly alternately wide and narrow planform carved into limestone of Pennsylvanian age in the Marble Falls Limestone formation (Figure 1). The exposed bedrock channel/floodplain system is 150 m wide, and is buffered on either side by high bluffs covered in dense Oak/Juniper forest. The high relief of the channel is controlled by intense bedrock jointing, and associated with diverse solution weathering features. As such, these characteristics make an ideal location to investigate the utility of the SfM-based terrain modeling process over a relatively small area, approximately 3.6 ha.

Image acquisition

Low altitude aerial photographs were collected with a Canon A480 compact digital camera (6.17 × 4.55 mm CCD sensor, 10.0 megapixel resolution) affixed to a unique helium-filled blimp, an Allsopp Skyshot helikite© (Vericat *et al.*, 2009). The helikite was released on 100 m of control line and walked around the study area to collect photographs covering the study area. We concentrated our imagery comparisons on the south half of the channel where access was allowed by the State Park administration. We found that the moderate wind conditions may have aided the SfM topographic process, as imagery of the same areas from several different angles became possible as the helikite was pushed in different semi-random directions beyond our simple survey lines. However, the effects of wind

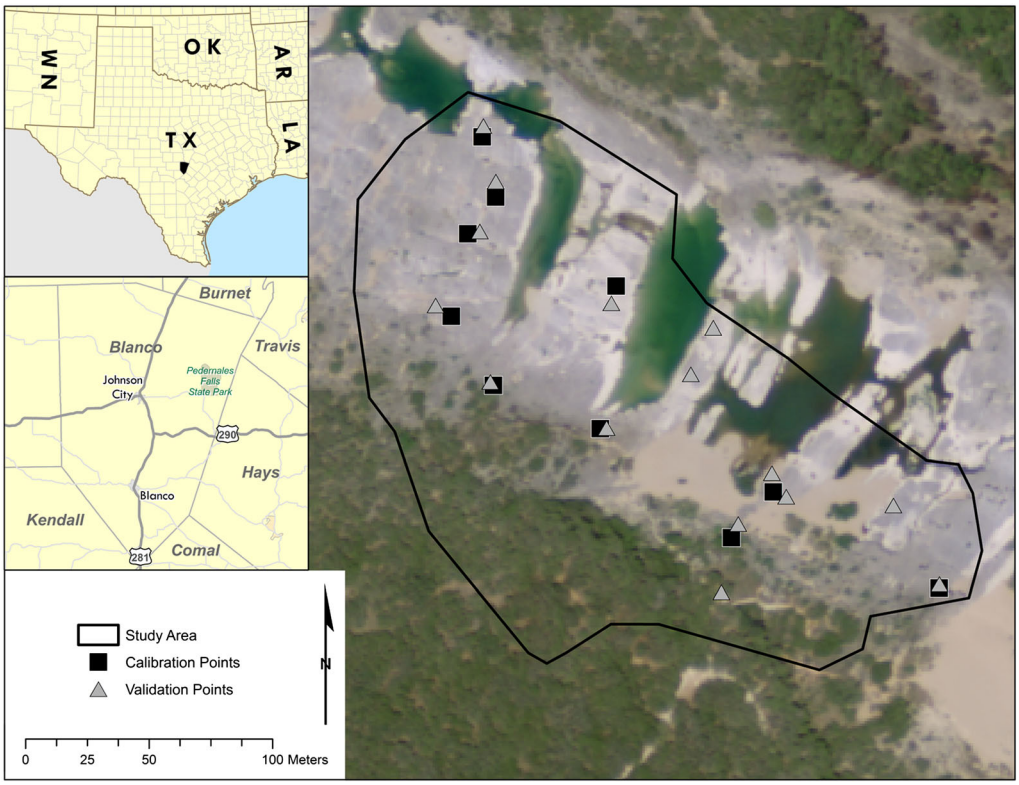

Figure 1. Overview of study area and GPS data collection locations. This figure is available in colour online at wileyonlinelibrary.com/journal/espl

and movement also limited the height of the helikite to an average of 40 m, with heights reaching a maximum of 70 m and as low as 10 m. The camera used in this study had an effective resolution of 10 megapixels that translated to ground resolutions of between 1 cm and 10 cm. The camera was programmed to capture three photographs every 10 s, which provided substantial overlap in sequential photographs, which is essential for the image matching algorithms used in SfM.

Global positioning system data collection and processing

We used a Trimble GeoXH, GPS unit to collect ground reference coordinates on 26 March 2011. GPS data was collected by averaging 180 real-time corrected positions per point feature. To ensure quality, the GPS was set to only collect locations with a maximum position dilution of precision (PDOP) ≤ 4 and 3D GPS mode. The data were then post-processed by applying differential corrections from eight dual frequency continuously operating reference stations (CORS; managed by the National Geodetic Survey) and Cooperative CORS using the GPS Analyst extension for ArcMap to derive the best position estimate for all ground control points. This post-processing resulted in 25 ground reference points, with a planimetric positional accuracy ranging from 0.06 m to 0.08 m ($\mu = 0.07$ m; $\sigma = 0.007$ m) and vertical uncertainties ranging from 0.08–0.16 m. Horizontal coordinates (X,Y) were referenced to UTM Zone 14 N, WGS 84, while GPS Z-values were referenced to the North American Vertical Datum 1988 (NAVD88) using a Geoid03 separation for orthometric height comparison with the LiDAR data.

SfM point cloud extraction and geographic projection

From the original image collection, we removed photographs that were blurred, outside the study area, or duplicated other images. The resulting 304 photographs that provided the best coverage of the study area were selected and processed using the Photosynth desktop application. This produced a three-dimensional reconstruction of photographs and a point cloud of features that were present in the photographs. Utilizing a free third party application, SynthExport (http://synthexport.codeplex.com), the point cloud was downloaded as a PLY (Polygon File Format) file. Preliminary editing of the raw point cloud was performed in MeshLab (free to download at http://meshlab.sourceforge.net/) to remove a small number of extraneous points that were clearly errors. The point cloud consisted of 554 308 points in an arbitrary, relative and internally consistent Cartesian coordinate system.

Rather than first placing ground targets into the imaged area we initially produced the point cloud and then revisited the site to collect GPS points. Ten points were selected based on our ability to identify the surface feature in the SfM point cloud and navigate directly to the feature in the field to record the GPS position. These ten GPS feature positions were used as ground control points to facilitate a full 3D coordinate transformation and an additional 15 points were collected for validation. We used the open-source software program JAG3D (http://javagraticule3d.sourceforge.net/) to perform the seven-parameter 3D transformation from the SfM Cartesian coordinates to GPS-observed UTM coordinates. The transformation was applied to entire point cloud resulting in root mean squared errors (RMSE) of 0.442 m in the X direction, 0.458 m in the Y direction, and 0.185 m in the Z (vertical) direction. The remaining 15 GPS points were used to test the accuracy of the transformation in the Z direction. The Z values for the 15 validation points were compared against a natural neighbor interpolated surface created from the georeferenced SfM data using a 0.5 m cell size. Results indicate a near 1:1 fit between SfM and GPS GCP and validation points (Figure 2).

LiDAR data collection and processing

The LiDAR data were acquired in spring and early summer of 2006 with an Optech 2050 airborne system. The data acquisition was part of a larger initiative to provide federal emergency management agency (FEMA) compliant elevation data for specific areas within the larger capital area council of governments (CAPGOG) in central Texas. Acquisitions were designed to provide a relatively high-density dataset of mass points suitable for development of contours required for hydraulic/hydrological model development, flood mitigation assessment, and environmental impact analysis. These data are available by request from CAPCOG (www.capcog.org).

The multiple-return datasets were delivered as .LAS files in the State Plane 4023 (Survey Feet), NAD83 and NAVD88 (US Foot) coordinate systems. The point cloud density of the LiDAR data was 0.33 points/m^2. We re-projected the LiDAR

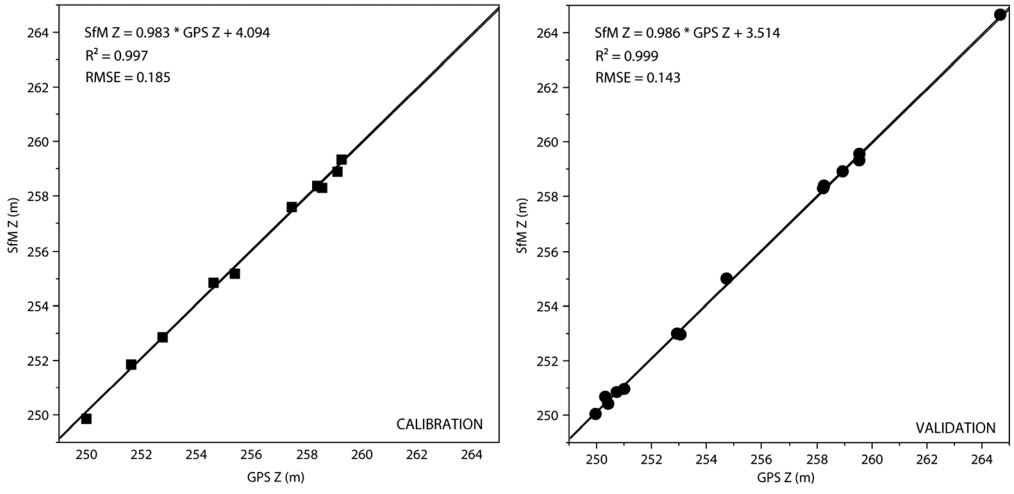

Figure 2. Calibration (left) and validation (right) plots of the fit between projected SfM Z-values and GPS observed orthometric height.

data to the UTM coordinate system for our study and adjusted vertical units to meters. Additionally, since the SfM approach only provides first surface Z-values (i.e. unlike LiDAR, SfM does not detect the ground beneath vegetation unless there are canopy gaps), we used first return LiDAR points for comparisons and to generate elevation surfaces.

SfM, LiDAR, and GPS comparisons

A full quantitative analysis of the accuracy and precision of the SfM approach to mapping topography is not the end goal of this communication. However, we can make an initial comparison between terrain produced by SfM photogrammetry and that measured by GPS and aerial LiDAR. Therefore, we compared the agreement between the SfM, GPS, and LiDAR datasets to assess relative differences between data acquisition methods. Since neither the LiDAR nor the SfM points are exactly spatially-coincident with the GPS point observations, we extracted the nearest point neighbor for each dataset (i.e. SfM and LiDAR points nearest in spatial proximity to each GPS point were used for comparison). Results of these comparisons are provided in Table I.

The horizontal and vertical accuracies of the SfM and LiDAR datasets were both within a reasonable level of accuracy. The occasionally large difference between the LiDAR and GPS validation points is likely due to the relatively sparse sampling density of the LiDAR acquisition (0.33 points/m^2), whereas the SfM point cloud was much more dense (10.8 points/m^2). Based on the values presented in Table I, we believe the level of accuracy for both the LiDAR and SfM datasets was sufficient for direct comparison of SfM and LiDAR. We performed this comparison by spatially-joining the SfM features directly to the LiDAR dataset, where each LiDAR point is compared based on the SfM point closest in spatial proximity.

In light of these considerations, we performed a comparison of SfM and LiDAR Z-values based on spatial proximity, just as we compared both dataset Z-values with the GPS validation points. This analysis approach resulted in 30 486 observations (i.e. the number of first return LiDAR records in our study area dataset) for comparison. SfM points were spatially-joined to LiDAR points in the GIS. We then evaluated the agreement between the two datasets by subtracting LiDAR Z-values from SfM Z-values.

Results

The elevation surfaces produced from both the SfM and LiDAR datasets are presented in Figure 3. These preliminary SfM results clearly have better feature representation when compared with

Table I. Comparisons of independent GPS-observations with projected SfM and LiDAR datasets

Dataset (n = 15)	Mean Δ* X (StDev)	Mean Δ Y (StDev)	Mean Δ Z (StDev)	Mean distance to GPS point** (StDev)
SfM - GPS	–0.03 m (0.19)	0.05 m (0.26)	0.07 m (0.15)	0.21 m (0.25)
LiDAR - GPS	–0.04 m (0.32)	–0.03 (0.39)	0.51 m (0.18)	0.44 m (0.21)

*Mean Δ values were calculated by subtracting the GPS values from the dataset of comparison and averaging the entire dataset.
**Point comparisons were obtained by extracting the nearest spatial neighbor for the 15 GPS validation points.

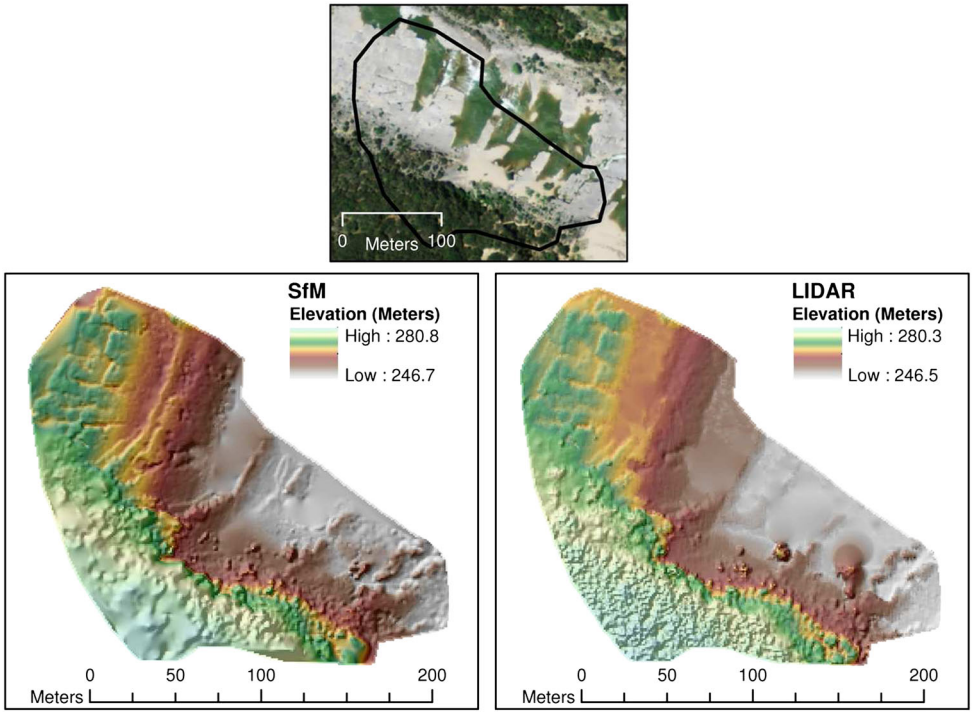

Figure 3. Merged elevation/hillshade surfaces for both the SfM (left) and LiDAR (right) datasets. The top figure is an aerial image showing the location of these surfaces.

this specific LiDAR dataset given the differences in point densities. Given the magnitude of difference in densities, a quantitative comparison of SfM Z-values relative to a LiDAR-derived elevation model would include significant interpolation in some areas where LiDAR returns were not present.

Results of the SfM-LiDAR comparisons are presented in Figure 4. The average distance between individual SfM and LiDAR points was 0.27 m ($\sigma = 0.25$ m). The mean difference of SfM and LiDAR Z-values within the study area was 0.60 m (+/- 1.08). Regression of SfM to LiDAR Z-values resulted in a 97% explanation of variance present in the LiDAR dataset. We acknowledge that the relationship is not 1:1 for all points within each dataset, particularly for those points outside elevation range of our training dataset (250–259.2 m). It is just beyond the upper limit of our calibration data that the 1:1 line begins to deviate from the regression line, though the deviation is relatively small.

A map of the error distribution between the two datasets is provided in Figure 5. Inspection of Figure 5 provides an opportunity to assess spatially the accuracy of the SfM approach relative to LiDAR. Of particular note is the light area at the south-western section of the study area. This area is comprised of topographically-varying features such as trees, large boulders, and sand. Further, the SfM point-cloud density is lower for this region of our study area as our research objectives were focused on the realism of a topographic bare-earth model.

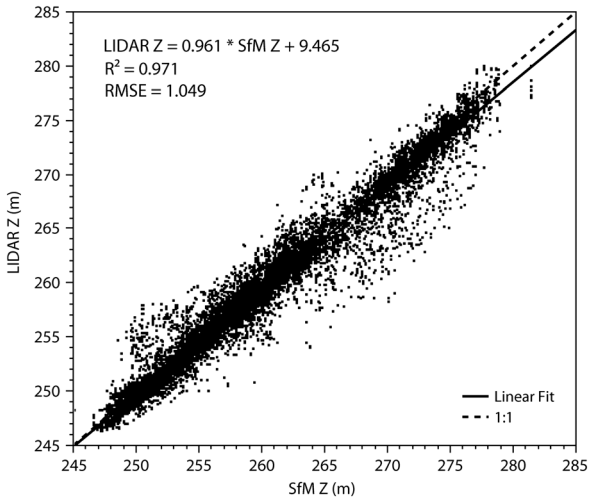

Figure 4. Scatterplot of LiDAR elevations vs. SfM elevations. The dashed line represents the 1:1 relationship. The solid line is the best-fit least squares regression line between the SfM elevations and those from LiDAR.

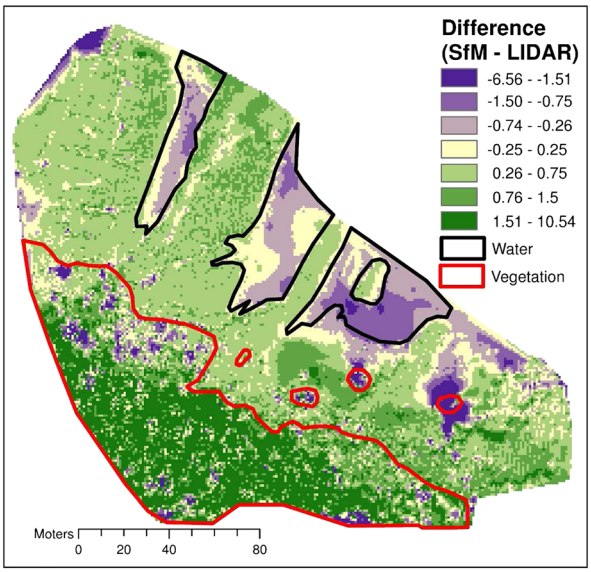

Figure 5. Distribution of SfM and LiDAR elevation differences. This figure is available in colour online at wileyonlinelibrary.com/journal/espl

Discussion

Structure from motion is appealing as a method because the less stringent requirements on image acquisition geometry and the high level of automation of the geometric solution and camera calibration. This could allow for both off-the-shelf and archival camera systems to be potential data sources. Furthermore, the ease of use of this highly automated approach could drastically reduce the cost and facilitate the production of high resolution Digital Elevation Models. We suspect that traditional photogrammetry would have generated similar accuracy results to our own, assuming that it could be accomplished from a similarly close-range platform as our helikite system. We note that Rango *et al.* (2009) found that unconstrained imagery acquired from a powered UAS was difficult to use in standard, traditional photogrammetry packages. Getting high-quality camera positions for close-range UAS aerial platforms can be difficult because most of these platforms (Helikites, small remote-controlled planes) cannot lift both cameras and high-resolution dGPS. Furthermore, Rango *et al.* (2009) found that traditional digital photogrammetry software is not well suited to unstructured image acquisition geometries and an additional step was needed which involved external image mosaicking software based on the same image matching techniques used in SfM. This would therefore suggest that an increased use of image matching technology is required in the production of topography from unconstrained imagery either with traditional photogrammetry or SfM approaches.

For the purposes of mapping topography from a low-altitude platform acquiring non-metric imagery in a preliminary fashion, we have found that SfM can generate aerial LiDAR-like accuracy and precision or better (roughly one point per square decimeter) for a non-vegetated surface (Figures 6 and 7). Under ideal flying conditions, a wide range of instrument heights, and high-contrast topographic surfaces, our extracted point clouds have densities closer to lower-resolution terrestrial laser scanning (TLS) than to aerial LiDAR (Brasington, 2010), with some point clouds approaching one point per square centimeter, particularly with new dense point cloud SfM software. For many applications, the slightly lower spatial resolution of the current helikite-generated points may outweigh the tremendous cost of TLS systems. The acquisition of a TLS is two or three orders of magnitude more expensive than the helikite system. A traditional ground survey using a total station would be of similar cost to the helikite system, but the resulting topographic point density would be orders of magnitude less for similar field-effort. It is yet unclear how well SfM-derived DEMs would perform in advanced geomorphic applications such as change detection measured using DEMs of difference (Rumsby *et al.*, 2008; Wheaton *et al.*, 2010). More robust and quantitatively precise investigations under a range of geomorphic conditions will be necessary to establish the SfM-derived DEMs for these purposes.

The SfM approach has some drawbacks. The most fundamental one is the absence of a procedure or step which can remove non-linear deformations in the elevation point-cloud. SfM is in essence an automated image matching procedure which generates relative topography followed by a rigid seven-parameter transformation to map coordinates. From the perspective of the

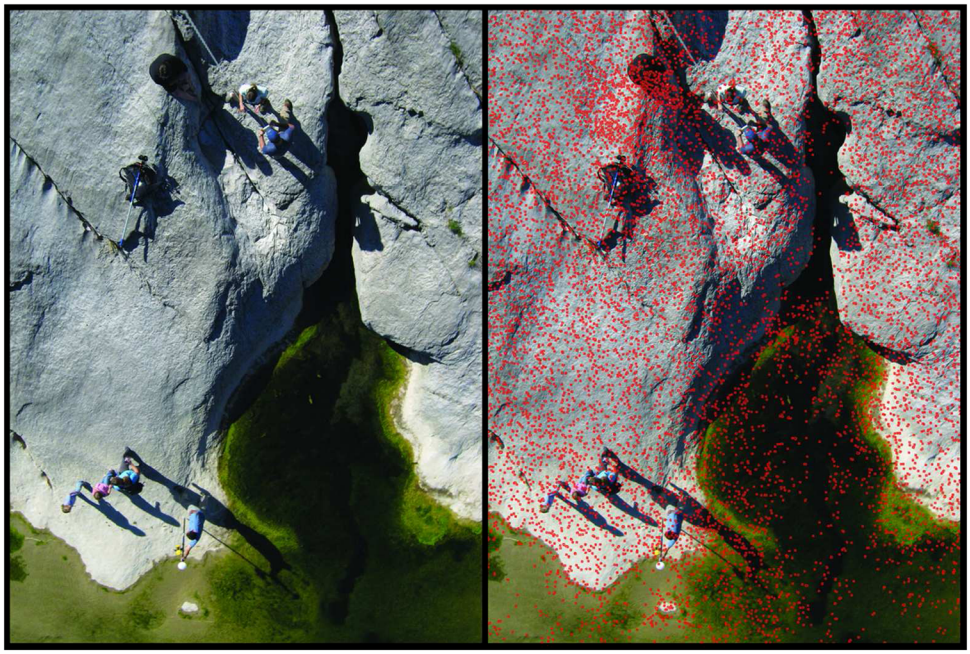

Figure 6. A close-up image taken with the helikite (left) and the same image overlaid with red topographic points derived using SfM (right). Even some submerged areas produce valid topographic points, as long as they are clear and have some spatial texture. In these frames such points are red, but cover the greenish-colored submerged bed. This figure is available in colour online at wileyonlinelibrary.com/journal/espl

Figure 7. Oblique view of a section of the Pedernales Falls research area georeferenced point cloud. The large linear black areas are deep water. This figure is available in colour online at wileyonlinelibrary.com/journal/espl

end-user, this process is extremely easy and simple. However, if the image matching process results in a point-cloud with a non-linear deformation, then the rigid seven-parameter transform used to register the point cloud to map coordinates will not remove such distortion. The presence of such non-linear distortions in the DEM could severely limit the potential accuracy of SfM photogrammetry. Certain software packages such as Photoscan by AgiSoft inc. do claim to have such a routine but its application is not a mandatory part of the SfM workflow and the results and associated quality have yet to be reported in the scientific literature. This is a crucial point which requires further investigation before SfM photogrammetry can be fully accepted as a standard method of topography generation. However, the empirical results presented here are promising and show that such deformations are not large. Another limitation is the dependence on image texture. As the image matching algorithm relies on image texture, areas of low image texture will yield poor point clouds. This could include areas of bare sand, snow, or other highly flat surfaces. Objects with different coloration and textures at different orientations, such as highly reflective surfaces, will likewise produce poor point clouds. This limitation is also characteristic of classic digital photogrammetry where automated matching is applied in order to construct dense DEMs (Fox and Gooch, 2001). In our study area, deep water absorbs and scatters light, reducing textural detail and yielding lower point densities. The SfM approach requires several images for any given point in order to both compute its location in the point cloud and to calibrate the camera parameters. How many pictures? The simple answer is: the more the better. We recommend a minimum of five or ten pictures, but areas with greater than these numbers (especially areas with subtle topography) should yield better digital topography. Also, the texture-based basis of the automated image matching means that a scale and resolution of imagery is needed that captures high detail. If the camera is too far away to make out a small bedrock step, or individual

tree leaves, it will not have the textural features required to accurately calculate a point cloud in that area. This probably means that SfM is most effective in small study areas, where moderate-quality cameras have sufficient resolution to capture detailed texture and are also light enough be carried on UASs, the tops of poles, or other hand-controlled platforms. Large area mapping with SfM would require both a platform that could easily move long distances and yet at the same time acquire very high-resolution imagery with little or no motion blur. We also recommend imagery at more than one distance from the topography if possible. Imagery from diverse ranges helps to reduce systematic distortions over large distances, whereas close-in imagery produces the fine-detail point clouds.

Improvements can definitely be made to the helikite/SfM system used in this first test. The Microsoft Photosynth software we used to extract topography performs what is known as 'sparse bundle adjustment'. The 3D point density is fairly low, as the primary aim of Photosynth is to rectify imagery, not reconstruct 3D surfaces. A much richer point density (dense point cloud reconstruction) can be extracted using advanced software. PMVS2 (freely available online), as one example, can take output data from Photosynth, as well as the original images, and can increase the number of points by ten or twenty times. We chose not to perform this more advanced reconstruction for this paper, as our intention was to highlight the results from the very simple Photosynth process. Dense point cloud reconstruction, however, would probably have increased point densities comparable with many TLS systems. The danger in increasing point densities and/or increasing the spatial area is that the number of images and points used in the bundle adjustment may overwhelm Photosynth, which was not originally designed for this type of use. An alternative approach would be to break the images and matched points into sections for bundle adjustment, and then remerge these sections together. This might be done using a different software system. Instead of Photosynth, Noah Snavely's Bundler software can perform a sparse bundle adjustment similar to Photosynth, but the outputs of Bundler can be split into more manageable sections using a package known as CMVS, and results from this software can then be densified in PMVS. Recently-released software products such as Agisoft PhotoScan, VirtualSfM, and Autodesk123D Catch incorporate many of these options into a straightforward interface. The advantage of using these more complex software system is the ability to manage the reconstruction of very large areas at high point density by distributing the bundle adjustment into many individual chunks that can individually be managed by standard desktop computers. Researchers should be careful, however, about always desiring extremely dense point clouds. Point clouds from terrestrial laser scanning, for example, can be extremely difficult to work with from a computational standpoint. Therefore, the needed point density should be part of the research design process and should be a requirement of specific research questions.

Another possible extension to the SfM topographic reconstruction is the automatic orthorectification of the original images. Photosynth calculates camera parameters (such as camera location and direction). While these parameters are in the same initial relative coordinate system as is the topographic point cloud, they could, in principle, be transformed to an absolute coordinate system along with the point cloud. After the point cloud has been converted to a DEM, the camera parameters can then be used to project the original images onto the DEM. As the DEM was made directly from these images, the orthorectification should be of extremely high quality. The commercial package Photoscan by Agisoft Inc. uses a SfM process similar to Bundler that both creates dense point clouds and orthorectifies the individual images. Another option would be to replace the ground control points collected using ground-based GPS with a GPS associated with the camera(s) used. As the camera parameters are calculated along with the point cloud, the transformation from a relative to an absolute coordinate system could use these platform based GCPs rather than ground GCPs; such was the approach of Welty *et al.* (2010), and it is one of the options in Photoscan. The disadvantage of this approach is that some platforms (helikites, UASs) are not able to carry large differential GPS systems, so the positional accuracy of the GPS becomes a potential issue. A third extension could be the possible use of a high-definition (HD) videocamera rather than using individual camera frames taken at some time interval. While HD videocameras are of lower resolution than individual camera frames, the fact that many more images are being captured means that there is far more overlap between images. Faster-moving platforms such as fixed-wing UASs (Dunford *et al.*, 2009) or low-flying aircraft might be able to use HD cameras to deal with the multiple-frame overlap required by the SfM process. If viable, this approach would allow already-existing aerial video footage to be converted to three-dimensional landscapes given the right conditions.

While a complete cost-benefit analysis of the SfM approach compared with other topography data collection approaches is beyond the scope of this study, some potential uses are immediately evident. Very small area, fine resolution topographic studies would benefit from the SfM approach immediately. Such applications might include fluvial features such as gravel river bed particle analysis, bar and bank forms, woody debris geometry, and small- and medium-sized channel 3D morphology. Many of these studies could be accomplished with simple hand-held cameras. The introduction of higher platforms, such as the helikite and UAS platforms, allows a much larger number of topographic features to be measured. Rather than expensive platforms, another option is to have many people taking images with several cameras. This 'flash mob' approach seems like a reasonable tactic for extracting 3D environments over small areas in a short amount of time. Disaster response (floods, hurricanes, debris flows), for example, would be helped by providing access to high-resolution 3D data quickly. Sending out a group determined to take large numbers of pictures of the area with many cameras should produce useful SfM-derived data at very low cost. For small study areas, it may possible to build topographic DEMs purely from ground-based imaging. By taking ground photos from a variety of angles and ranges, SfM may be useful not only from a cost-savings and ease-of-construction perspective, but also in avoiding the problems of shadowing and drop-out common to terrestrial and aerial laser scanning. In research areas of tens or hundreds of meters, we have found that putting a camera on the end of a several-meter long pole (such as a painter's pole), and having the camera take pictures at fixed intervals can result in imagery with both high resolution and broad extent.

We strongly suspect that it should be possible to combine ground-based and close-range aerial images in an individual SfM process to negate many of the disadvantages of LiDAR, such as the line-of-sight obscurations that happen due to vegetation and other complex objects. Having many different cameras perspectives greatly increases the point cloud density and (we suspect) the individual point precision and having a combination of ground and aerial camera placements should increase the robustness of topographic mapping. Having such a combination of perspectives might also reduce large-area distortions while at the same time allowing high resolution detail.

The ease of use and wide applicability of the SfM software raises some interesting possibilities. It may be possible to extract useful 3D topography from motion pictures and video products. While these are usually of lower resolution than

individual photos, they have the advantage of consistent lighting, many overlapping frames and images, and a long history. Some 'impossible' geomorphic measurements, such as the precise measurement of woody debris over large and difficult to access areas, may be well-served by SfM. Our testing of SfM from a low-altitude instrument platform found the technique to be extremely simple-to-use, and had high topographic quality and precision, at least in areas with 'complex' surfaces. Further tests of this approach in other environments and with different platforms would be very useful to geomorphology as a whole; there are environments where this technique may be failure-prone, for example, 'smooth' surfaces such as uniform snow and sand may be very difficult surfaces from which to extract SfM topographic datasets. Nevertheless, these tests could be completed at essentially no cost but sweat equity, and further software development may improve the SfM approach even further. From a more quantitative perspective, we strongly suggest that the geomorphic community undertake rigorous comparative studies between SfM-derived topographic datasets and datasets constructed though other high-resolution means (such as total-station survey, RTK GPS, and laser scanning) in a wide range of geomorphic environments and under different imaging conditions (some examples include Rosnell and Honkavaara, 2012; James and Robson, in press). It is important that the geomorphic community establish a baseline knowledge of accuracy, precision, and resolution we should expect by this methods under different circumstances. Once this knowledge is established, we expect SfM to be a powerful tool for future geomorphic studies.

Conclusions

This study tested the utility of the SfM photogrammetric approach in a bedrock fluvial setting from low-altitude aerial imagery, and found it to be of comparable accuracy and precision to aerial LiDAR data but with a greatly enhanced ease-of-use and a significant reduction in labour time. Remote sensing in many parts of geomorphology would greatly benefit from approaches like SfM that take low cost images and convert them, with little or no technical training and low-cost or free software, to high quality point clouds and eventually to topographic and orthophoto datasets. The approach is straightforward, and takes very little time for raw data collection and data processing. Recent advances in software power and usability should allow exactly that, provided the resulting topographic datasets are of high quality. Moreover, the potential exists to apply this approach to historic, archival, and non-standard imagery sources such as motion pictures, and to extend photogrammetry to a larger number of platforms such as very small UASs and groups of individuals with their own cameras. The geomorphic community needs to investigate the accuracy, resolution and precision of SfM-derived topographic datasets in a wide range of geomorphic environments.

Acknowledgements—We would like to extend our thanks to the Capital Area Council of Governments for providing free access to the LiDAR dataset used in our study and Texas Parks and Wildlife, and the staff at Pedernales State Park for providing access to the park. This manuscript benefited from the comments of Joe Wheaton and two anonymous reviewers.

References

Alho P, Kukko A, Hyyppa H, Kaartinen H, Hyyppa J, Jaakkola A. 2009. Application of boat-based laser scanning for river survey. *Earth Surface Processes and Landforms* **34**(13): 1831–1838.

Baily B, Collier P, Farres P, Inkpen R, Pearson A. 2003. Comparative assessment of analytical and digital photogrammetric methods in the construction of DEMs of geomorphological forms. *Earth Surface Processes and Landforms* **28**(3): 307–320.

Bird S, Hogan D, Schwab J. 2010. Photogrammetric monitoring of small streams under a riparian forest canopy. *Earth Surface Processes and Landforms* **35**(8): 952–970.

Brasington J. 2010. From grain to floodplain: hyperscale models of braided rivers. *Journal of Hydraulic Research* **48**(4): 52–53.

Butler JB, Lane SN, Chandler JH. 2001. Characterization of the structure of river-bed gravels using two-dimensional fractal analysis. *Mathematical Geology* **33**(3): 301–330.

Butler JB, Lane SN, Chandler JH, Porfiri E. 2002. Through-water close range digital photogrammetry in flume and field environments. *The Photogrammetric Record* **17**(99): 419–439.

Carbonneau PE, Lane SN, Bergeron NE. 2003. Cost-effective non-metric digital photogrammetry and its application to a study of coarse gravel surfaces. *International Journal of Remote Sensing* **24**(14): 2837–2854.

Chandler J. 1999. Effective application of automated digital photogrammetry for geomorphological research. *Earth Surface Processes and Landforms* **24**(1): 51–63.

Chandler J, Ashmore P, Paola C, Gooch M, Varkaris F. 2002. Monitoring river-channel change using terrestrial oblique digital imagery and automated digital photogrammetry. *Annals of the Association of American Geographers* **92**(4): 631–644.

Chandler JH, Mills JP, Robson S, Lane SN. 2003. Comment on 'Hillslope topography from unconstrained photographs' by A.M. Heimsath and Hany Farid. *Mathematical Geology* **35**(3): 347–350.

Dietrich JT. 2010. Visualizing small-scale geomorphic features using 3D models derived from Microsoft Photosynth. Poster presentation at 41st Binghamton Geomorphology Symposium, Columbia, SC, USA, 15–17 October.

Dietrich JT, Fonstad MA, Courville BC, Jensen JL, Carbonneau PE. 2011. High resolution, automated, low-cost topographic mapping with Microsoft Photosynth. Paper Presentation, Annual Meeting of the Association of American Geographers, Seattle, WA, USA, 12 April.

Dowling TI, Read AM, Gallant JC. 2009. Very high resolution DEM acquisition at lost cost using a digital camera and free software. 18th World IMACS / MODSIM Congress, Cairns, Australia 13–17 July, 2479–2485.

Dunford R, Michel K, Gagnage M, Piegay H, Tremelo ML. 2009. Potential and constraints of unmanned aerial vehicle technology for characterization of Mediterranean riparian forest. *International Journal of Remote Sensing* **30**(19): 4915–4935.

Fonstad MA, Marcus WA. 2010. High resolution, basin extent observations and implications for understanding river form and process. *Earth Surface Processes and Landforms* **35**(6): 680–698.

Fonstad MA, Dietrich JT, Courville BC, Jensen JL. 2011a. Lighter-than-air blimps as a testbed for river remote sensing techniques. Poster presentation, Annual Meeting of the American Geophysical Union, San Francisco, CA, USA, 16 December.

Fonstad MA, Dietrich JT, Courville BC, Jensen JL, Carbonneau PE. 2011b. High resolution, low-cost 3D riverscape mapping using field photography. Paper Presentation, Annual Meeting of the American Fisheries Society, Seattle, WA, USA, 8 September, 2011.

Fonstad MA, Dietrich JT, Courville BC, Jensen JL, Carbonneau, PE. 2011c. Topographic Structure from Motion. Paper Presentation, Annual Meeting of the American Geophysical Union, San Francisco, CA, USA, 9 December, 2011.

Fox AJ, Gooch MJ. 2001. Automatic DEM generation for antarctic terrain. *The Photogrammetric Record* **17**(98): 275–290. DOI: 10.1111/0031-868x.00183.

Gimenez R, Marzolff I, Campo MA, Seeger M, Ries JB, Casali J, Alvarez-Mozos J. 2009. Accuracy of high-resolution photogrammetric measurements of gullies with contrasting morphology. *Earth Surface Processes and Landforms* **34**(14): 1915–1926.

Hancock G, Willgoose G. 2001. The production of digital elevation models for experimental model landscapes. *Earth Surface Processes and Landforms* **26**: 475–490.

Heritage G, Hetherington D. 2007. Towards a protocol for laser scanning in fluvial geomorphology. *Earth Surface Processes and Landforms* **32**(1): 66–74.

Höfle B, Rutzinger M. 2011. Topographic airborne LiDAR in geomorphology: a technological perspective. *Zeitschrift Für Geomorphologie* **55**: 1–29.

Hohenthal J, Alho P, Hyyppa J, Hyyppa H. 2011. Laser scanning applications in fluvial studies. *Progress in Physical Geography* **35**(6): 782–809.

James MR, Robson S. Straightforward reconstruction of 3D surfaces and topography with a camera: accuracy and geoscience application. *Journal of Geophysical Research*. In press.

Lane SN. 2000. The measurement of river channel morphology using digital photogrammetry. *The Photogrammetric Record* **16**(96): 937–957.

Lane SN. 2003. Editorial: the generation of high quality topographic data for hydrology and geomorphology: new data sources, new applications and new problems. *Earth Surface Processes and Landforms* **28**(3): 229–230.

Lane SN, Westaway RM, Hicks DM. 2003. Estimation of erosion and deposition volumes in a large, gravel-bed, braided river using synoptic remote sensing. *Earth Surface Processes and Landforms* **28**(3): 249–271.

Lane SN, Widdison PE, Thomas RE, Ashworth PJ, Best JL, Lunt IA, Smith GHS, Simpson CJ. 2010. Quantification of braided river channel change using archival digital image analysis. *Earth Surface Processes and Landforms* **35**(8): 971–985.

Lowe DG. 1999. Object recognition from local scale-invariant features. In *The Proceedings of the Seventh IEEE International Conference on Computer Vision* 1150–1157.

Marcus WA, Fonstad MA. 2008. Optical remote mapping of rivers at sub-meter resolutions and basin extents. *Earth Surface Processes and Landforms* **33**: 4–24.

Marzolff I, Poesen J. 2009. The potential of 3D gully monitoring with GIS using high-resolution aerial photography and a digital photogrammetry system. *Geomorphology* **111**(1–2): 48–60.

Miller PE, Kunz M, Mills JP, King MA, Murray T, James TD, Marsh SH. 2009. Assessment of glacier volume change using ASTER-based surface matching of historical photography. *IEEE Transactions on Geoscience and Remote Sensing*, **47**(7): 1971–1979. DOI: 10.1109/Tgrs.2009.2012702.

Notebaert B, Verstraeten G, Govers G, Poesen J. 2009. Qualitative and quantitative applications of LiDAR imagery in fluvial geomorphology. *Earth Surface Processes and Landforms* **34**(2): 217–231.

Rango A, Laliberte A, Herrick JE, Winters C, Havstad K, Steele C, Browning D. 2009. Unmanned aerial vehicle-based remote sensing for rangeland assessment, monitoring, and management. *Journal of Applied Remote Sensing* **3**(1): 033542. DOI: 10.1117/1.3216822

Rosnell T, Honkavaara E. 2012. Point cloud generation from aerial image data acquired by a Quadrocopter type micro unmanned aerial vehicle and a digital still camera. *Sensors* **12**(1): 453–480.

Rumsby, BT, Brasington J, Langham JA, McLelland SJ, Middleton R, Rollinson G. 2008. Monitoring and modelling particle and reach-scale morphological change in gravel-bed rivers: applications and challenges. *Geomorphology* **93**(1–2): 40–54.

Smith MJ, Chandler J, Rose J. 2009. High spatial resolution data acquisition for the geosciences: kite aerial photography. *Earth Surface Processes and Landforms* **34**(1): 155–161. DOI: 10.1002/Esp.1702.

Snavely N. 2008. Scene reconstruction and visualization from internet photo collections. Doctoral thesis, University of Washington.

Snavely N, Seitz SM, Szeliski R. 2006. Photo tourism: exploring photo collections in 3D. *ACM Transactions on Graphics* **25**(3): 835–846.

Snavely N, Seitz SM, Szeliski R. 2008. Modeling the world from internet photo collections. *International Journal of Computer Vision* **80** (12): 189–210.

Templeton RC, Vivone ER, Mendez-Barroso LA, Rango A, Laliberte A, Saripalli S. 2010. Emerging technologies for ecohydrological studies during the North American monsoon in a Chihuahuan desert watershed. Poster H53B-1014. 2010 American Geophysical Conference Annual Conference, San Francisco, USA.

Verhoeven GJJ. 2009. Providing an archaeological bird's-eye view – an overall picture of ground-based means to execute low-altitude aerial photography (LAAP) in archaeology. *Archaeological Prospection* **16** (4): 233–249.

Verhoeven GJJ, Loenders J, Vermeulen F, Docter R. 2009. Helikite aerial photography – a versatile means of unmanned, radio controlled, low-altitude aerial archaeology. *Archaeological Prospection* **16**(2): 125–138.

Vericat D, Brasington J, Wheaton J, Cowie M. 2009. Accuracy assessment of aerial photographs acquired using lighter-than-air blimps: low-cost tools for mapping river corridors. *River Research and Applications* **25**(8): 985–1000.

Welty E, Pfeffer WT, Ahn Y. 2010. Something for everyone: quantifying evolving (glacial) landscapes with your camera. Poster IN33B-1314. 2010 American Geophysical Union Annual Conference, San Francisco, USA.

Westaway RM, Lane SN, Hicks DM. 2003. Remote survey of large-scale braided, gravel-bed rivers using digital photogrammetry and image analysis. *International Journal of Remote Sensing* **24**(4): 795–815.

Wheaton JM, Brasington J, Darby SE, Sear DA. 2010. Accounting for uncertainty in DEMs from repeat topographic surveys: improved sediment budgets. *Earth Surface Processes and Landforms* **35**(2): 136–156.

Wolf PR, Dewitt BA. 2000. *Elements of Photogrammetry with Applications in GIS*, 3rd edn. McGraw-Hill Professional: Boston, Massachusetts.